*CHAPTER 6*

# LIQUID CIRCULATION

In this chapter, the pseudo-homogeneous fluid concept is clarified and a pseudo-homogeneous liquid circulation model is developed. A new two-fluid liquid circulation model is proposed, and the problems of the previous two-fluid models are discussed. Based on a known expression for the radial turbulent viscosity distribution in single-phase pipe flows and an empirical description for the radial gas holdup distribution in bubble columns, analytical expressions for the liquid velocity profiles are obtained from the two models proposed by this work. these are easy and fast to use, and of course have no convergence problems. The velocity profiles calculated by these models are shown to agree well with reported experimental data both for low viscosity and high viscosity fluids. This implies that there may exists a strong analogy for turbulent properties such as the eddy viscosity distribution, between multi-phase and single-phase systems.

The pseudo-homogeneous fluid model is the simpler, but an optimization of gas holdup distribution may be needed. The two-fluid model gives more exact results using known or measured gas holdup distribution parameters.

## 6.1 Introduction

Liquid circulation induced by rising bubbles is also one of the important characteristics of bubble column reactors. Almost all the hydrodynamic, transport and

mixing properties such as gas holdup, interfacial area, mass and heat transfer coefficients and dispersion coefficients influence and depend on it. Especially, liquid circulation is directly a decisive factor for determining the mixing properties of the reactors which may seriously affect final reaction yield and product selectivity. Therefore, the exact prediction of the flow structure is necessary for effective design and scale-up of bubble columns and in recent years considerable experimental and theoretical effort has been directed towards research on the circulation behavior.

In bubble columns, the liquid rises in the bubble wakes in the central portion, having a maximum velocity near the column axis, and flows downwards in the outer annulus. There is an inversion point, at which the time averaged liquid velocity is zero, located between the column center and the wall. The location of this inversion point depends on the properties of the gas-liquid system and the operating conditions. Since the liquid velocity at the wall is zero, there must exist a maximum downward velocity in the outer annulus.

Radial liquid velocity profiles above the entrance region have been measured by many investigators (*e.g.* Pavlov, 1965; Rietema and Ottengraf, 1970; Miyauchi and Shyu, 1970; Hills, 1974; Ulbrecht and Baykara, 1981; Walter and Blanch, 1983; Franz *et al.*, 1984; Menzel *et al.*, 1990; Yu and Kim, 1991), using various methods such as tracer bubbles or particles, Pitot tubes and micro-hot-film anemometers. These studies have shown that the normalized profiles for the time averaged axial liquid velocity in ordinary bubble columns operating in the turbulent region are relatively stable, if the system properties are similar.

Many models have been proposed to analyze and predict the liquid circulation based on a known radial distribution of void fraction. Rietema and Ottengraf (1970) gave an analysis for viscous liquid flow which is only applicable to laminar flow conditions. Viswanathan and Rao (1984) obtained an analytical velocity profile only for inviscid fluids.

Miyauchi and Shyu (1970) proposed a basic equation of motion for the two-phase flow in bubble columns as follows,

$$\frac{1}{r}\frac{d}{dr}\left(r\mu_t\frac{du}{dr}\right) - \frac{dP}{dz} + \rho_L g\left(1-\varepsilon_G\right) \qquad (6.1)$$

where $u$ should be the mixture velocity, since this equation was based on the pseudo-homogeneous fluid or "one-fluid" concept in which the two-phase flow system was considered as a single-phase (mixture) flow with a radially varying density (Miyauchi and Shyu, 1970).

On the basis of Equation (6.1), Miyauchi and Shyu (1970) developed a liquid circulation model with the eddy or turbulent viscosity, $\mu_t$, as adjustable parameter. The model neglected the molecular viscosity and assumed constant eddy viscosity over the entire cross-section, leading to large deviations near the wall.

Equation (6.1) was used by many investigators later. Walter and Blanch (1983), Yang *et al.* (1986) and Orell (1992) used Equation (6.1) and the same assumptions as Miyauchi and Shyu (1970). Therefore, similar models and results were obtained. In these models, the inversion point for liquid velocity had to be given in advance. For example, the inversion points for the air-water system and high viscosity systems were given at $r/R \approx 0.7$ and 0.5-0.6 respectively.

Hills (1974) also used Equation (6.1), but assumed that the turbulent viscosity or "momentum dispersion coefficient" was proportional to the product of local gas and liquid holdups, $\varepsilon_G(1-\varepsilon_G)$, instead of a constant. Numerical solutions were obtained from the model. Clark *et al.* (1987) obtained numerical solutions for a force balance equation also based on the pseudo-homogeneous fluid concept together with the turbulent mixing length theory. They used the wall shear stress as an adjustable parameter and assumed that the eddy mixing length in bubble columns was the same as that in singe-phase pipe flows where an empirical radial distribution of the mixing length is available. In addition, they assumed that the liquid velocity was zero at a finite distance from the wall, instead of at the wall. This distance had to be determined in advance.

Menzel *et al.* (1990) measured the turbulence intensity and Reynolds shear stress in bubble columns with the aid of a newly developed experimental technique and

proposed a model, using the gas-liquid slip velocity and the so-called Reichardt constant as adjustable parameters in addition to the empirical profiles of eddy viscosity and gas holdup.

However, for most of the pseudo-homogeneous models mentioned above, they mixed with the two-fluid concept when determining the liquid velocity (see section 6.2).

Unlike the work mentioned above, Anderson and Rice (1989) proposed a model using the two-fluid (or "separated flow") concept where the turbulent stress was considered to be locally varying and the classical turbulence theories of von Kármán and Prandtl were invoked in the central and the outer annulus regions respectively. This gave three analytical velocity expressions for the three flow zones in the radial direction: core, buffer and clear laminar wall layer. Several parameters in their model must be evaluated before the equations can be used. In addition, the model assumed the gas holdup profiles to be flat in the core and buffer zones respectively, and zero in the laminar layer near the wall, thereby introducing large errors close to the wall. Rice and Geary (1990) modified the two-fluid model by dividing the cross-section into a main flow zone and a bubble-free zone (near the wall) and used the Prandtl strain model for the two zones respectively. The division line between the main flow and bubble-free zone was assumed to coincide with the position of the maximum downward velocity. In addition, the Prandtl mixing length was assumed to be proportional to the product of the mean bubble size and the local void fraction, while the mean bubble size had to be given before using the model. Later, Geary and Rice (1992) have modified their own model by using the principle of energy minimization.

However, the above two-fluid models used the very questionable assumption that the shear stresses in liquid and gas phases are equal. This makes the equation of motion in the two-fluid models the same as that of the pseudo-homogeneous models and thus the two concepts were mixed also in this case (see the section about the two-fluid model).

In this chapter, the pseudo-homogeneous fluid and the two-fluid concepts will

be clarified. Models for the axial liquid velocity profiles are developed using the two concepts respectively. Analytical expressions are obtainable for these models, based on a known turbulent viscosity distribution in single-phase pipe flows and an empirical model for the radial gas holdup distribution in bubble columns.

## 6.2 Pseudo-Homogeneous Fluid Model

### 6.2.1 Equation of motion

According to the pseudo-homogeneous fluid concept, the two-phase flow system is considered as one fluid (single-phase) flow, but the density of this fluid varies in the radial direction and equals $\rho_L(1-\varepsilon_G)$ (Miyauchi and Shyu, 1970). Thus, for the steady axial-symmetric single-phase flow in cylindrical coordinates (Bird *et al.*, 1960), when the radial and angular velocities are disregarded and the change of pressure in the radial direction is negligible, the equation of motion can be written as

$$-\frac{1}{r}\frac{\partial(r\tau)}{\partial r} = \frac{dP}{dz} + \rho_L g(1-\varepsilon_G) \tag{6.2}$$

where $\varepsilon_G$ is radially varying local gas holdup and $\tau$ is the shear stress related to the time-averaged axial mixture velocity, $u$, as defined in Equation (6.1). This equation is the more general form of Equation (6.1) and has widely been used in describing the liquid circulation in bubble columns.

Equation (6.2) is simple, convenient and easy to be used for obtaining the velocity profile, $u$. However, the problem is how to consider and determine the liquid velocity from the solution of this equation.

There have been two ways suggested to do this. The first considers the velocity, $u$, as the real liquid velocity in a two-phase system (*e.g.* Miyauchi and Shyu,

1970; Hills, 1974; Ueyama and Miyauchi, 1979; Yang *et al*, 1986; Orell, 1992). According this idea, the net liquid flow rate is calculated by

$$Q_L = 2\pi \int_0^R r(1-\varepsilon_G) u dr \tag{6.3}$$

Obviously, this equation will be correct only when $u = u_l$. However, the consideration, $u_l = u$, is contradictory to the basic concept from which the equation of motion, Equation (6.2), has been derived.

The second approach is to consider as if only the liquid phase exists in the system and then $u_l = u$ (Walter and Blanch, 1983; Clark *et al.*, 1987). Hence, the net liquid flow rate is

$$Q_L = 2\pi \int_0^R r u dr \tag{6.4}$$

This consideration agrees, of course, with the pseudo-homogeneous fluid assumption. It may be more reasonable, since a given point in a bubble column may temporarily be occupied by either gas or liquid, but the probability for this being liquid is usually higher since normally $\varepsilon_G < 0.5$. In addition, the viscous shear stress, which usually governs the equation of motion, has its main contributed from the liquid, as discussed in the next section. Besides these, Equation (6.2) can also be obtained assuming the two-phase flow as a single-phase liquid flow system with a radially varying gravity $g(1-\varepsilon_G)$.

Thus, the pseudo-homogeneous fluid concept may be corrected by imagining it as a pure liquid flow in a radially varying gravity field, instead of having a fluid of radially varying density. The basic equation of motion is then expressed by Equation (6.2) with the constraint condition given by Equation (6.4). The velocity in question is the liquid velocity, $u_l$.

The liquid flow in a bubble column, as discussed in Chapter 3, is usually in the turbulent regime due to the disturbance of bubbles. However, in the zone close to the wall, the effect of molecular viscosity may be important. Generally the shear stress for a Newtonian fluid is expressed by

$$\tau = -\rho_L(\nu_t + \nu_L)\frac{du_l}{dr} \tag{6.5}$$

where $u_l$ is the local time-averaged axial liquid velocity and $\nu_t$ is the turbulent viscosity indicating the turbulent intensity of the flow.

The axial change of liquid velocity above the entrance region of a column is usually negligible. Hence, integrating Equation (6.2) over the whole cross section area, one can obtain

$$-\frac{dP}{dz} = \frac{2\tau_w}{R} + \rho_L g(1-\bar{\varepsilon}_G) \tag{6.6}$$

Substituting this into Equation (6.2), it can be rewritten as

$$-\frac{1}{r}\frac{d(r\tau)}{dr} = -\frac{2\tau_w}{R} + \rho_L g(\bar{\varepsilon}_G - \varepsilon_G) \tag{6.7}$$

where $\bar{\varepsilon}_G$ is the average gas holdup over the whole cross-section.

The eddy viscosity in Equation (6.5) is a very important parameter for such equations of motion as Equation (6.2) or Equation (6.7), and is usually not known a priori for bubble columns. For viscous fluids in single-phase flows, both the eddy viscosity itself and the impact of the molecular viscosity are known to be radially variant. In the central zone, the eddy viscosity may be large enough so that the molecular viscosity may be disregard, but in the zone close to the wall, the molecular viscosity has a determining effect on the flow. The constant eddy viscosity assumption made in some models (*e.g.* Miyauchi and

Shyu, 1970; Ueyama and Miyauchi, 1979; Yang *et al*, 1986; Orell, 1992) is not generally valid and may become a main source of error in the models.

It is difficult to determine the eddy viscosity distribution in bubble columns directly. However, a lot of data and expressions concerning the eddy viscosity distribution for single-phase pipeline flows are available in the literature (*e.g.* Reichardt, 1951; Deissler, 1955; Rannie, 1956; Hinze, 1959; Mizushina and Ogino, 1970; Davies, 1972; Datta, 1993). If the turbulence in bubble columns and in pipes is analogous, it is reasonable to assume that the distribution of eddy viscosity in a bubble column may follow the same pattern as that in single-phase pipe flows. This concept is confirmed by the recent measurements of Menzel *et al.* (1990) who found that the eddy viscosity profiles in a bubble column can be described by an equation proposed by Reichardt (1951) for single phase flows:

$$\frac{\nu_t}{\nu_L} = k_R \tilde{R}(1+2\phi^2)(1-\phi^2) \tag{6.8}$$

where $\tilde{R} = R\hat{u}/\nu_L$, is the Reynolds number (or the dimensionless radius of the column) based on the friction velocity, $\hat{u}$, which is defined as $(|\tau_W|/\rho_L)^{1/2}$. The parameter, $k_R$, is the "Reichardt constant" defined by Menzel *et al.* (1990). For high turbulence flow in pipes, $k_R$ is nearly a constant of 0.07 (Hinze, 1959). However, the value of $k_R$ for single-phase flows may also depend on the average flow Reynolds number (Datta, 1993).

The radial gas holdup profile in a bubble column is found to be quite complicated. It depends heavily, not only on the physical and chemical properties of the system, but also on the static liquid height and the type of gas distributor (Ueyama *et al.*, 1980). Axial variation of the profile for gas void fraction may be found in bubble columns, especially close to the entrance and outlet regions (Menzel, 1990). The coalescence properties of the system also strongly influence the profile as reported by Fan (1989) and Menzel *et al.* (1990). Up to now, the local gas holdup, even above the entrance region of a bubble column, can not be determined theoretically from operating conditions and bulk chemical proper-

ties. In general, one has to resort to empirical expressions. Several power law functions have been used to describe the radially varying gas holdup (Ueyama and Miyauchi, 1979; Clark *et al.*, 1987; Menzel *et al.*, 1990) and the most commonly used is

$$\varepsilon_G = \bar{\varepsilon}_G \frac{m+2}{m+2-2c}(1-c\phi^m) \tag{6.9}$$

where $\phi$ is the dimensionless radial coordinate, $r/R$. The parameters $m$ and $c$ have to be determined for each individual case, and the variation in $c$ gives possibilities for both zero and non-zero values of gas void fraction at the wall. $c = 1$, including complete liquid wetting of the wall, is the most common since it seems to coincide with physical intuition.

### 6.2.2 Expression of liquid velocity

Knowing the radial profile of the gas holdup, the first integration of Equation (6.7), combining with Equation (6.8), gives the velocity gradient:

$$\frac{d\tilde{u}_l}{d\phi} = \frac{A\phi - [(Bc)/(m+2-2c)](\phi - \phi^{m-1})}{2k_R\tilde{R}(\alpha-\phi^2)(\beta+\phi^2)} \tag{6.10}$$

where the condition of an axial-symmetric liquid velocity profile has been used and $\tilde{u}_l$ is the dimensionless liquid velocity, $\tilde{u}_l = u_l/u_{l0}$. The dimensionless parameters, $\alpha$, $\beta$, $A$ and $B$, in the above equation are defined as

$$\alpha = \frac{1}{4}\left[1+\sqrt{9+8/(k_R\tilde{R})}\right]$$
$$\beta = \frac{1}{4}\left[-1+\sqrt{9+8/(k_R\tilde{R})}\right] \tag{6.11}$$

and

$$A = \frac{-R\tau_W}{\rho_L \nu_L u_{l0}}$$

$$B = \frac{gR^2\bar{\varepsilon}_G}{u_{l0}\nu_L} \tag{6.12}$$

It is worth noting that the term in the above equations taking into account the effect of shear stress at the wall, $A$, should always have a positive value instead of a negative one, as found in the models of Walter and Blanch (1983) and Yang *et al.* (1986). This is because the flow direction near the wall is opposite to the main flow direction and the wall shear stress $\tau_W$ should then be negative.

Knowing $\nu_t = 0$ at $\phi = 1$ from physical intuition or Equation (6.8), the parameter, $A$, can further be obtained from Equation (6.10) as

$$A = \left.\frac{d\tilde{u}_l}{d\phi}\right|_{\phi=1} \tag{6.13}$$

Equation (6.13) shows that the parameter, $A$, is only the velocity gradient at the column wall. From this equation and the definition of the dimensionless radius, $\tilde{R}$, it can be expressed by

$$\tilde{R} = \sqrt{ARe_0/2} \tag{6.14}$$

Then, the liquid velocity profile can be obtained by integrating Equation (6.10), noting that $\tilde{u}_l(1) = 0$, as follows

$$\bar{u}_l = \frac{1}{2k_R\bar{R}}\left[AI_1 - \frac{Bc}{m+2-2c}\left(I_{m-1} - I_{m-1}\right)\right]_0^1 \tag{6.15}$$

where

$$I_0 = \frac{1}{\alpha+\beta}\left[\frac{1}{2\sqrt{\alpha}}\ln\left(\frac{\sqrt{\alpha}-\phi}{\sqrt{\alpha}-\phi}\right)+\frac{1}{\sqrt{\beta}}\arctan\left(\frac{\phi}{\sqrt{\beta}}\right)\right]$$

$$I_1 = \frac{1}{2(\alpha+\beta)}\ln\left(\frac{\beta+\phi^2}{\alpha-\phi^2}\right)$$

$$I_2 = \frac{1}{(\alpha+\beta)}\left[\frac{\sqrt{\alpha}}{2}\ln\left(\frac{\sqrt{\alpha}+\phi}{\sqrt{\alpha}-\phi}\right)-\sqrt{\beta}\arctan\left(\frac{\phi}{\sqrt{\beta}}\right)\right] \tag{6.16}$$

$$I_3 = -\frac{1}{2(\alpha+\beta)}\left[\alpha\ln(\alpha-\phi^2)+\beta\ln(\beta+\phi^2)\right]$$

and

$$I_q = \frac{1}{2}\left\{\left[1-(k_R\bar{R})^{-1}\right]I_{q-4}+I_{q-2}\right\}-\frac{\phi^{q-3}}{q-3}, \quad q \geq 4 \tag{6.17}$$

Equation (6.15) is derived on the basis of the basic equation of motion stemming from the pseudo-homogeneous liquid flow concept, together with the known turbulent viscosity and gas holdup distributions. It analytically expresses the mean axial velocity profile in bubble columns and is easy to use, since it avoids solving any differential or integral equations.

The net liquid flow rate as expressed by Equation (6.4), can, from Equation (6.15), be rewritten as

$$\tilde{u}_L = \frac{1}{2k_R\tilde{R}}\left[AI_3 - \frac{Bc}{m+2-2c}\left(I_3 - I_{m-3}\right)\right]_0^1 \tag{6.18}$$

where $\tilde{u}_L$ is the dimensionless superficial liquid velocity, $u_L/u_{l0}$.

If the maximum liquid velocity, $u_{l0}$, is known, parameters $A$ and $B$ can be determined by the boundary condition, $\tilde{u}_l(0) = 1$, and Equation (6.18). Then the average gas holdup contained in parameter $B$ is determined. Similarly, if the average gas holdup is known, the maximum liquid velocity can be determined.

## 6.3 Two-Fluid Model

### 6.3.1 Equation of motion

Obviously, the pseudo-homogeneous concept is simple, but not satisfactory as a physical concept. In addition, as will be seen from the discussion later, the parameter, $m$, in the liquid circulation model using the pseudo-homogeneous fluid concept, may need to be tuned to experimental data.

An improvement, both in the physical concept sense and from a practical point of view, can be obtained by using the two-fluid concept for two-phase flow systems (Rietema, 1982; Svendsen and Torvik, 1990; Jakobsen, 1993). The general equations of motion for the two-fluid model can be expressed by

$$\varepsilon_i \rho_i \frac{Du_i}{Dt} = -S_i + W_i + F_{ji} \tag{6.19}$$

where $S_i$ and $W_i$ are the stress and body forces acting on phase $i$ ($i = L$ or $l$ referring to liquid, or $i = G$ or $g$ referring to gas) per unit dispersion volume. $F_{ji}$ is the interaction force with which phase $j$ acts on phase $i$ ($F_{ji} = -F_{ij}$) per unit dispersion volume.

According to Rietema (1982), $S_i = \nabla \cdot \varepsilon_i T_i$, where $T_i$ represents the stress tensor acting on phase $i$ per unit volume of phase $i$ and $T_i = \tau_i + P_i\delta$ ($\tau_i$ is the shear stress tensor and $\delta$ is the unit tensor). For the flow in the gravity field, Equation (6.19) can be rewritten for the two phases respectively as

$$\varepsilon_L \rho_L \frac{Du_l}{Dt} = -\nabla \cdot \varepsilon_L \tau_l - \nabla(\varepsilon_L P) + \varepsilon_L \rho_L g + F_s$$

$$\varepsilon_G \rho_G \frac{Du_g}{Dt} = -\nabla \cdot \varepsilon_G \tau_g - \nabla(\varepsilon_G P) + \varepsilon_G \rho_G g - F_s \qquad (6.20)$$

where $\varepsilon_L = 1-\varepsilon_G$, $u_l$ and $u_g$ are the linear liquid and gas velocity vectors, $\tau_l$ and $\tau_g$ are the shear stress tensors of the liquid and gas phases respectively, $F_s$ is the generalized interfacial drag force and $P$ is the local pressure in the continuous phase (here the local pressure in the dispersed phase has been assumed to equal that in continuous phase). It should be noted that the velocity, $u_g$, is in reality the bubble velocity, instead of the gas velocity inside bubbles.

The shear stress tensor of the liquid phase, $\tau_l$, it can be determined without problem. When changes only in the radial direction are considered, it can be expressed by Equation (6.5). However, there has been a lot of discussion as to the determination of the gas phase shear stress tensor, $\tau_g$. For the shear stress of dispersed phase (here the bubble phase), $\tau_g$ is not the shear stress tensor inside individual bubbles, but can be conceived as the result of such interactions as collisions, mechanical friction and coalescence, between the dispersed bubbles. Of course, it is not obvious how to incorporate coalescence in the momentum equations of a dispersed two-phase flow system. However, the shear stress of the dispersed phase can be considered to be negligible for low coalescing systems (Rietema, 1982). At low gas holdup, Lahey (1990) disregarded $\tau_g$.

Non-zero values of $\tau_g$ have been assumed in turbulent gas-liquid flows (Torvik, 1990; Jakobsen, 1993), but it was found that $\tau_g \ll \tau_l$ according to an analysis of flow continuity. This is reasonable, since $\tau_g$ is the consequence of interactions between bubbles while $\tau_l$ results from the interaction of eddies. In the column

central zone where the effect of liquid eddy motion is significant, there usually is a large number of bubbles, and the interactions such as collisions and mechanical friction between bubbles are strengthened by the turbulent motion of liquid eddies. However, these bubble-bubble interactions may still be much weaker than the interactions between eddies, not only due to the interaction intensity (liquid has higher momentum than gas at the same velocity), but also due to the interaction probability. In the zone very close to the wall, the turbulent shear stress of the liquid phase is weak and the liquid molecular shear stress becomes dominant. However, here the bubble number density is very small or nearly bubble-free (Anderson and Rice, 1989; Rice and Geary).

Thus, it may be concluded that $\tau_g < \tau_l$ in bubble columns. For a steady axial-symmetric flow system where the radial and angular velocities are ignored, adding the two equations included in Equation (6.20), noting that $\rho_G < \rho_L$ and considering that the pressure change in the radial direction is usually small, the following equation can be obtained.

$$-\frac{1}{r}\frac{\partial}{\partial r}\left[r\left(1-\varepsilon_G\right)\tau\right] = \frac{dP}{dz}+\left(1-\varepsilon_G\right)\rho_L g \tag{6.21}$$

where $\tau_l$ has been written as $\tau$ to be accordance with Equation (6.5).

Since this is a two-fluid model, the net liquid flow rate should be expressed by Equation (6.3).

It is necessary to point out that Anderson and Rice (1989) and Rice and Geary (1990) proposed two models for the liquid circulation by using the two-fluid concept and the assumption, $\tau_g = \tau_l$ or the shear stress of the dispersed gas phase equaling that of the continuous liquid phase. From the above discussion, it is seen that this assumption may be very questionable. Under this assumption, the same equation of motion as for the pseudo-homogeneous model, Equation (6.2), was finally obtained, but the two-fluid concept was still retained for determining the net liquid flow rate. Hence, their models were not of real two-fluid and also mixed the two concepts.

Using the same manipulations as in the pseudo-homogeneous fluid model, Equation (6.21) becomes

$$-\frac{1}{r}\frac{d}{dr}\left[r(1-\varepsilon_G)\tau\right] = -\frac{2\tau_W}{R}+(\bar{\varepsilon}_G-\varepsilon_G)\rho_L g \tag{6.22}$$

### 6.3.2 Expression of liquid velocity

Using Equation (6.9) with $c = 1$ and combining Equation (6.5), the first integration of Equation (6.22) yields an expression for the liquid velocity gradient,

$$\frac{d\tilde{u}_l}{d\phi} = \frac{\left(A_1-B_1+B_1\phi^m\right)\phi}{\left(C+\phi^m\right)\left(\alpha-\phi^2\right)\left(\beta+\phi^2\right)} \tag{6.23}$$

where

$$A_1 = \frac{A}{\varepsilon_{G0}k_R\tilde{R}}, \quad B_1 = \frac{B}{m\varepsilon_{G0}k_R\tilde{R}}, \quad C = \frac{1-\varepsilon_{G0}}{\varepsilon_{G0}} \tag{6.24}$$

$$\varepsilon_{G0} = \bar{\varepsilon}_G(m+2)/m \tag{6.25}$$

and $\tilde{u}_l(1) = 0$ has been used.

When $m$ is an even number (axial-symmetric distribution of gas holdup) and $\varepsilon_{G0} \le 0.5$, an analytical expression for the liquid velocity can be obtained as

$$\tilde{u}_l = \frac{[A_1-B_1(1+C)](J_1+J_2)+B_1J_3}{2(\alpha+\beta)} \tag{6.26}$$

where

$$J_1 = J_4 + \frac{1}{\alpha^{m/2} + C} \ln\left(\frac{\alpha - 1}{\alpha - \phi^2}\right)$$

$$J_2 = J_5 + \frac{1}{(-\beta)^{m/2} + C} \ln\left(\frac{\beta + \phi^2}{\beta + 1}\right) \tag{6.27}$$

$$J_3 = \ln\left[\frac{(\beta + \phi^2)(\alpha - 1)}{(\beta + 1)(\alpha - \phi^2)}\right]$$

$$J_4 = \sum_{i=1}^{m/2} \left[\frac{a_i \phi^{2i}}{iC} F\left(\frac{\phi^m}{C}, \frac{2i}{m}\right)\right]_1^{\phi}$$

(6.28)

$$J_5 = \sum_{i=1}^{m/2} \left[\frac{b_i \phi^{2i}}{iC} F\left(\frac{\phi^m}{C}, \frac{2i}{m}\right)\right]_1^{\phi}$$

$$F(z_1, z_2) = 1 + z_2 \sum_{k=1}^{\infty} (-1)^k \frac{z_1^k}{k + z_2} \tag{6.29}$$

and

$$a_i = [\alpha^i (1 + C\alpha^{-m/2})]^{-1}$$

(6.30)

$$b_i = -\{(-\beta)^i [1 + C(-\beta)^{-m/2}]\}^{-1}$$

If $\bar{\varepsilon}_G$ is given, the velocity, $\bar{u}_{l0}$, and the dimensionless wall velocity gradient, $A$,

can be calculated from the constraint condition, Equation (6.3), and the boundary condition, $\bar{u}_l(0) = 1$.

## 6.4 Results and Discussion

### 6.4.1 Pseudo-homogeneous model

#### *6.4.1.1 Effect of $k_R$*

According to the results of single-phase pipe flow, the value of the Reichardt constant, $k_R$, in Equation (6.8) is a constant of about 0.07 for fully developed turbulence, but may depend on the average flow Reynolds number (Hinze, 1959; Datta, 1993). In the model of Menzel *et al.* (1990), the Reichardt constant, $k_R$, was considered to be an adjustable parameter, and a value $k_R = 0.188$ was suggested for low viscosity liquids and $k_R = 0.30$ for high viscosity liquids.

In the present work, the dimensionless liquid velocity profiles corresponding to different values of $k_R$, in the wide range of 0.07-1.89, have been calculated at given values of the Reynolds number. At small values of the Reynolds number, the differences between the profiles for varying values of $k_R$ are apparent, as shown in Figure 6.1. From Figure 6.2, it is seen that the variations decrease with an increase in the Reynolds number and become insignificant in the middle section of the column. It is also seen that the larger the Reichardt constant, the sharper the peak of the reverse liquid flow. This is reasonable, because the larger the Reichardt constant, the larger the ratio of the turbulent viscosity and the molecular viscosity under a given turbulent intensity, as seen in Equation (6.8). This means the effect of the turbulent viscosity will dominate a wider region from the center to the wall. When the Reynolds number, $Re_0$, is larger than 1000 (in practical columns, $Re_0$ is usually larger than this value), the dimensionless liquid velocity profiles will nearly coincide. An exception is the region very close to the wall since the velocity gradients at the wall depend strongly on the values of $k_R$. In addition, when the shape of the gas holdup profiles becomes sharper ($m < 8$), the differences become even less.

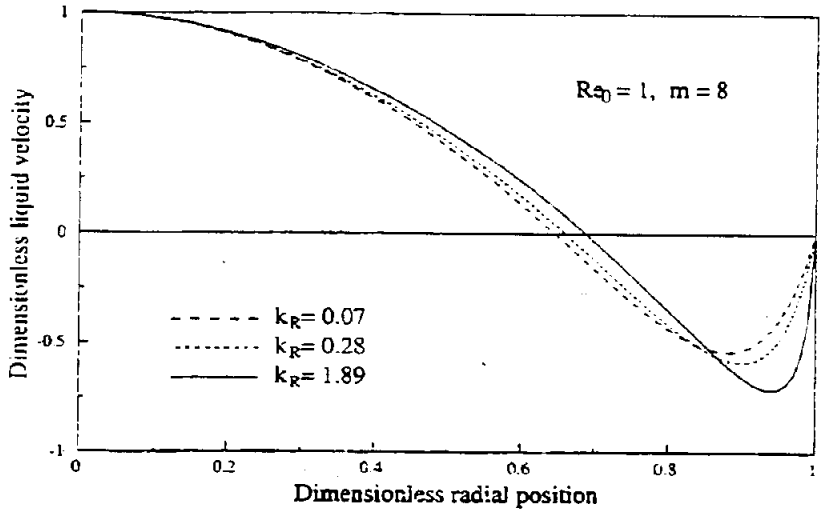


**Figure 6.1** Effect of $k_R$ on liquid velocity profiles for $Re_0 = 1$.

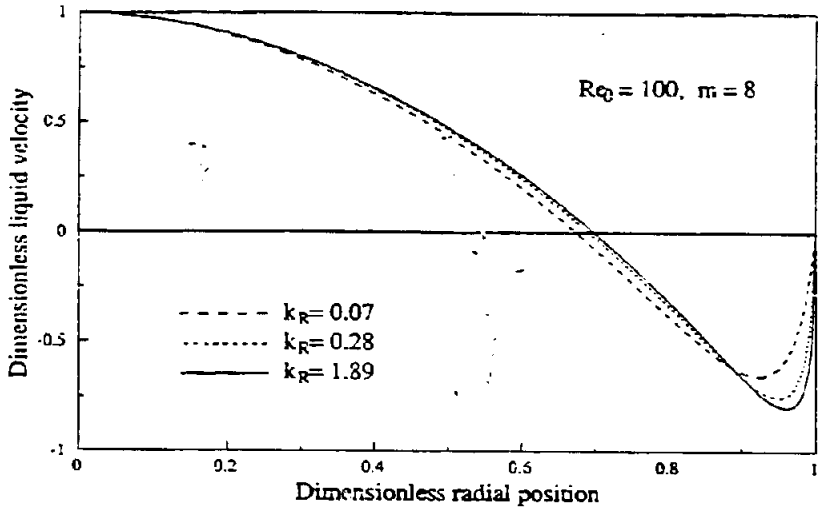


**Figure 6.2** Effect of $k_R$ on liquid velocity profiles for $Re_0 = 100$.

The above results leads to the conclusion that the shape of the dimensionless liquid velocity profile in systems operating in a practical Reynolds number region, is not sensitive to the value of the Reichardt constant. Hence, in what follows, a value of 0.07 is used for calculating the liquid velocity profiles. However, it should be kept in mind that the Reichardt constant can influence the value of the maximum liquid velocity, $u_{l0}$, and thereby the values of the parameters $A$ and $B$. A brief discussion of these parameters will be given later.

### 6.4.1.2 *Effect of* $Re_0$

Calculated dimensionless liquid velocity profiles for various values of the Reynolds number, $Re_0$, at given values of the Reichardt constant, $k_R$, and shape factor of gas void distribution, $m$, are shown in Figure 6.3 and Figure 6.4. The dimensionless liquid velocity profiles change significantly with the Reynolds number when the Reynolds number is small, but are more stable for large values of the Reynolds number ($Re_0 > 1000$). An exception again is the region close to the wall. This is caused by the increased significance of the molecular viscosity at the smaller Reynolds numbers, especially in the outer annulus. It is interesting to note that the inversion point for the liquid velocity predicted by this model is about 0.68-0.71 for the turbulent flow region in low viscosity liquids and moves closer to the center with decreasing Reynolds number or increasing influence of molecular viscosity. This agrees very well with the empirical model of Yang *et al.* (1986).

For high viscosity liquids, the value of $m$ is small. For example, $m = 1$, as suggested by Walter and Blanch (1983). The liquid velocity profiles for $m = 1$ are shown in Figure 6.4. When the Reynolds number is small, as is usually the case in high viscosity liquids, the profiles predicted by our model are in very good agreement with the data for the high viscosity fluid systems reported by Walter and Blanch (1983) and by Yang *et al.* (1986). Both the shape of the curve and the radial position of the maximum downward velocity of liquid ($\phi = 0.8$). This implies that the present model may be extrapolated also to cases with high viscosity liquids.

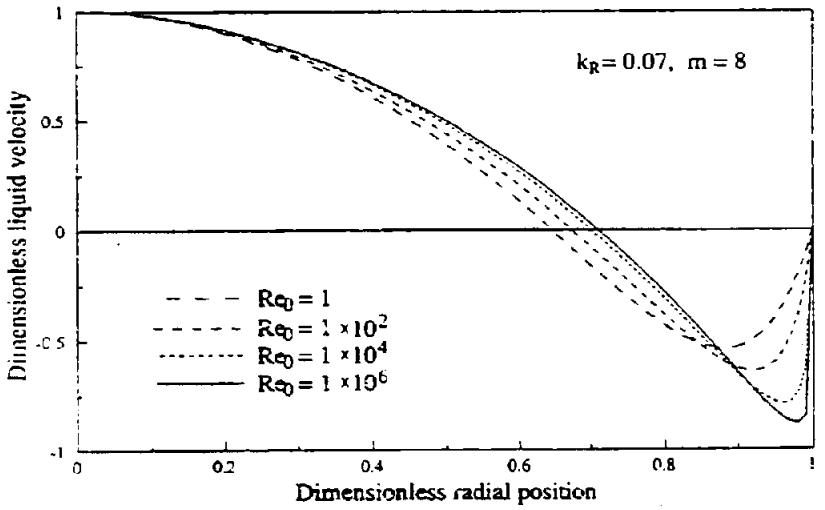


**Figure 6.3** Effect of $Re_0$ on the liquid velocity profiles for $m = 8$.

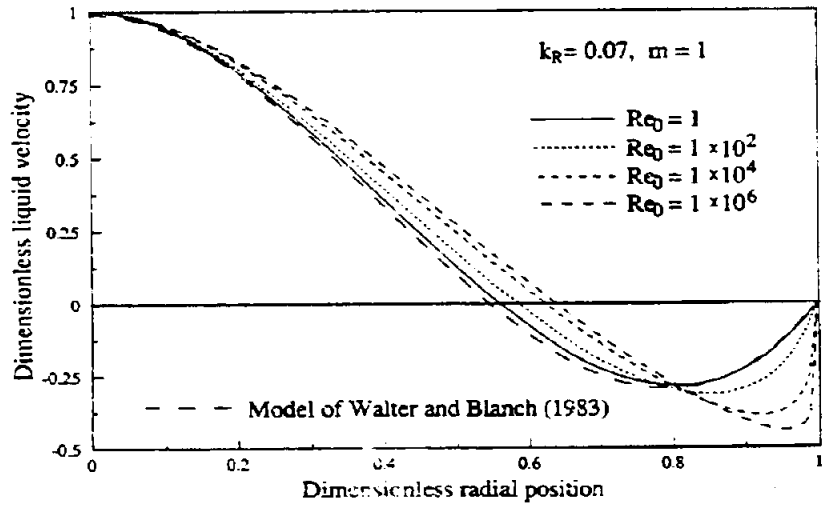


**Figure 6.4** Effect of $Re_0$ on the liquid velocity profiles for $m = 1$.

*6.4.1.3 Effect of holdup distribution*

As mentioned previously, prediction of the radial distribution of gas void fraction in bubble columns is very complicated and the values of the coefficient, $c$, and the shape factor, $m$, in Equation (6.9) depend on the individual case. This may be the reason why there is some controversy regarding these values even for high turbulence cases. Walter and Blanch (1983) and Yang *et al.* (1986) suggested that the profile of gas holdup should be parabolic ($c$ = 1 and $m$ = 1.8-2.3) in their models. Clark *et al.* (1987) considered that it may differ significantly from the parabolic shape at low gas superficial velocity. Kawase and Moo-Young (1987) suggested that $c$ = 1 and $m$ = 15 for a large bubble column of 5.5 m diameter, based on the experimental results of Koide *et al.* (1979). Menzel *et al.* (1990) from their experimental data suggested that $c$ = 0.5 and $m$ = 4 for the homogeneous flow regime and $m$ = 2 for the heterogeneous flow regime.

On the other hand, the measurements of Miyauchi and Shyu (1970) over a very wide range of gas superficial velocities ($u_G$ = 4.5-37.0 cm/s) showed that the values of $m$ and $c$ do not seem to be related to flow regimes, universally $c$ = 1 and $m$ = 8.

As seen above, taking $c$ = 1 is very common. This is because this value indicates that the void fraction at the wall is zero, which also coincides with physical intuition.

As can be seen from Figure 6.5 and Figure 6.6, the profiles of liquid velocity corresponding to different values of the shape factor, $m$, are very different even at high Reynolds numbers ($Re_0 = 10^6$). The smaller the value of $m$, the closer to the center the inversion point of liquid velocity and the smoother the profile near the wall. This coincides with general experimental observations: A sharp distribution of gas void fraction will be accompanied by a sharp profile in liquid velocity in the central portion of the column.

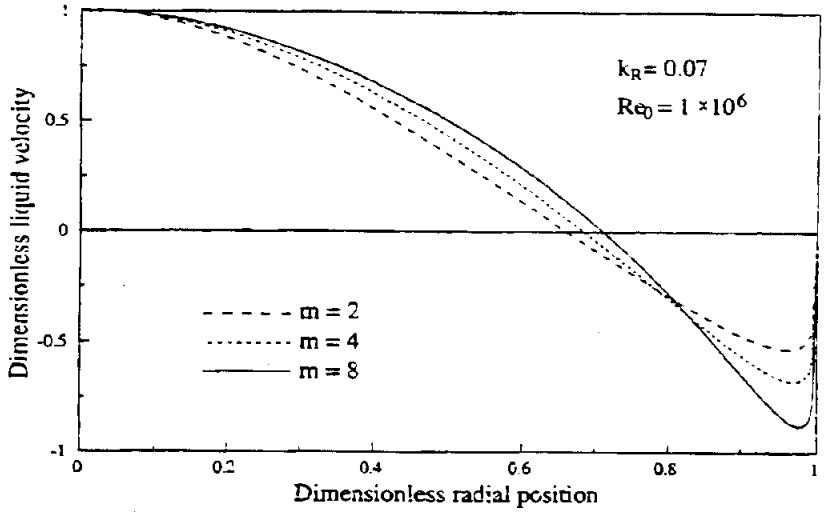


**Figure 6.5** Effect of $m$ on liquid velocity profiles for $Re_0 = 10^6$.

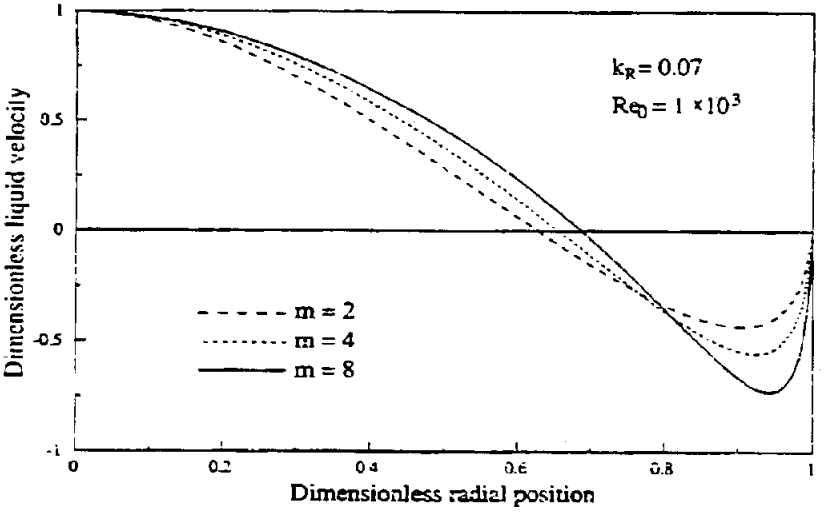


**Figure 6.6** Effect of $m$ on liquid velocity profiles for $Re_0 = 10^3$.

The coefficient, $c$, in Equation (6.9) has no effect on the dimensionless velocity profiles but makes the value of $B$ defined by Equation (6.12) change. This can be seen from Equation (6.10) and Equation (6.15): The profile of the liquid

velocity depends on the global value of $Bc/(m+2-2c)$, which is influenced by the different values of $c$. Since the value of $Bc/(m+2-2c)$ is given for a given system, this relationship presents a new way either to determine the value of $c$ from the known average gas holdup and the shape factor, $m$, or to predict the average gas holdup from the correct value of $c$ and the shape factor, $m$, like in the work of Kawase and Moo-Young (1987).

*6.4.1.4 Comparison with reported experimental results*

Figure 6.7 to Figure 6.10 show comparisons between the liquid velocity profiles calculated by the present model and experimental data for the fully developed turbulence cases ($Re_0 > 10000$), available in the literature. The measured maximum liquid velocities for the individual cases were used for the calculations, since the measured average gas holdups were not given.

It is seen that the model gives very good predictions both for coalescing and non-coalescing turbulent systems, and for the inner and the outer annulus. A value of $m = 8$ can be used for the cases where the superficial gas velocity is not too high (< 10 cm/s). This indicates that the expression for the radial gas holdup profiles proposed by Miyauchi and Shyu ($m = 8$) seems to be the most suitable for low viscosity fluids. For non-coalescing systems as shown in Figure 6.9, $m = 4$ or 2 may give better velocity predictions in the outer annulus, but $m = 8$ is still best for the core.

Figure 6.11 gives the predicted results and the reported data of Rietema and Ottengraf (1970) for a high viscosity system. It can be seen that the predicted results are quite good. This is reasonable, because (i) the flow may have the turbulent characteristics of a bubble column even with a high viscosity liquid due to the influence of bubbles, as mentioned previously, and (ii) it is the additive effect of the turbulent and the molecular viscosities which is considered by the model through Equation (6.8). For a highly viscous system the velocity gradient at the wall is low and the Reynolds number or dimensionless radius, $\tilde{R}$, is therefore small. This means that the effect of the molecular viscosity will become significant.

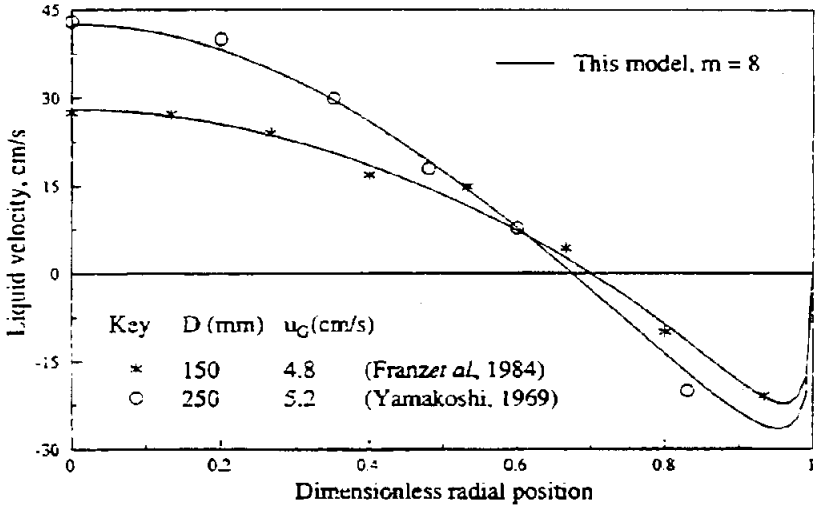


**Figure 6.7** Comparison with the data of Franz (1983) and Yamakoshi (1969).

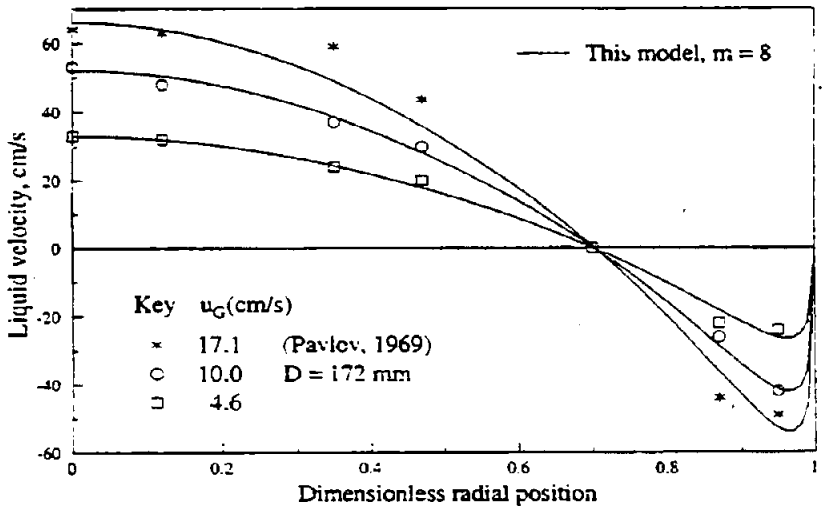


**Figure 6.8** Comparison with the data of Pavlov (1969).

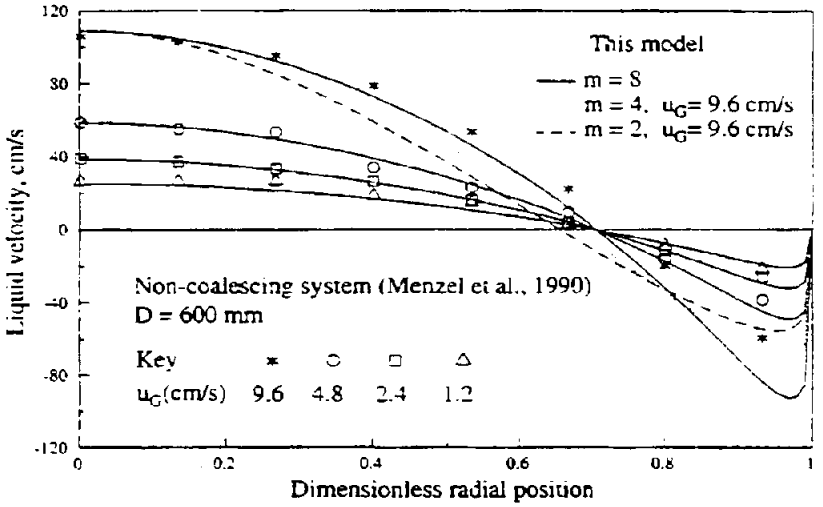


**Figure 6.9** Comparison with the data of Menzel *et al.* (1990) in a non-coalescing system.

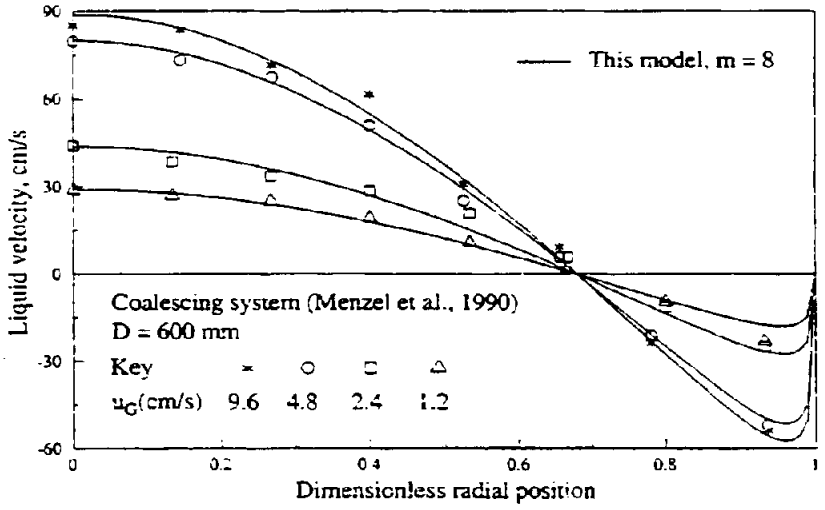


**Figure 6.10** Comparison with the data of Menzel *et al.* (1990) in a coalescing system.

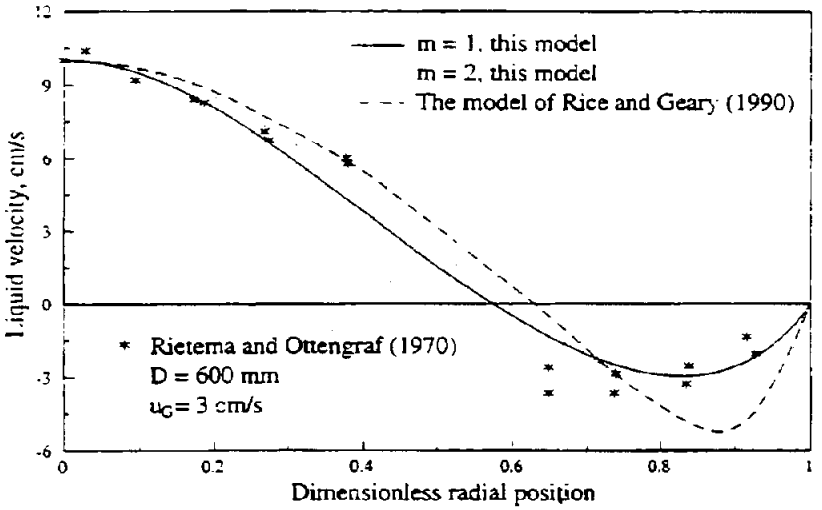


**Figure 6.11** Comparison with the data of Rietema *et al.* (1970) in a high viscosity liquid system.

### 6.4.2 Two-fluid model

#### *6.4.2.1 Effect of the Reichardt constant*

As in the pseudo-homogeneous model, the dimensionless liquid velocity profiles calculated by the two-fluid model are also insensitive to the Reichardt constant, $k_R$, but the maximum liquid velocity, $u_{l0}$ is considerably affected by the constant, as shown in Figure 6.12. The smaller the Reichardt constant, $k_R$, the larger the maximum liquid velocity, $u_{l0}$. For the air-water system, the position of the inversion point is independent of the Reichardt constant. This is also similar to the results for the pseudo-homogeneous model (when the Reynolds number, $Re_0$, is large, the inversion point is nearly independent of $k_R$).

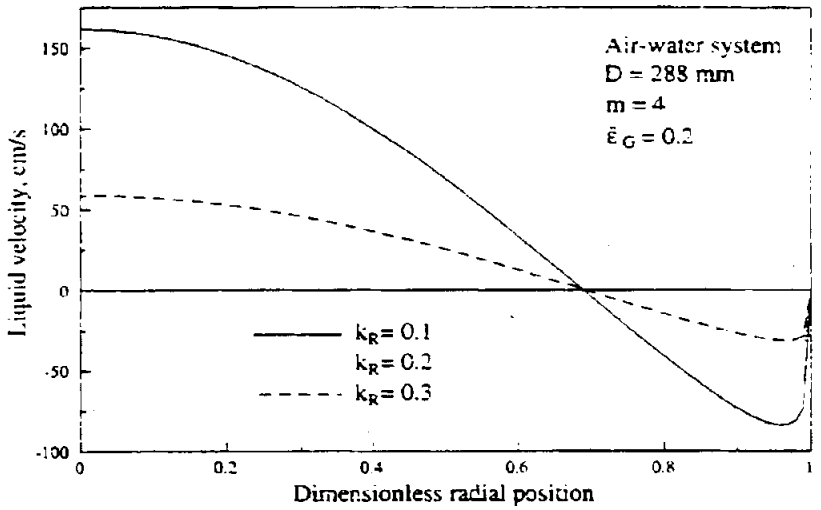


**Figure 6.12** Effect of $k_R$ on $u_l$.

For the two-fluid model, it is found that $k_R$ = 0.2 is suitable for low viscosity systems. This value agrees with that (0.188) obtained by Menzel *et al.* (1990).

### *6.4.2.2 Effects of m and D*

Figure 6.13 shows the effect of the gas holdup shape factor, $m$, on the liquid velocity profiles. It can be seen that the smaller the shape factor, the larger the maximum liquid velocity and the closer to the column axis the inversion point. As discussed before this is reasonable since increased non-uniformity of gas holdup distribution will strengthen the liquid circulation.

The effect of column diameter can also be seen in Figure 6.13. The liquid circulation intensity will increase with the column diameter. This is definitely reasonable, because the larger the column diameter the smaller the wall effect. This trend also agrees with the empirical and semi-theoretical correlations of Koide *et al.* (1979), Kraume and Zehner (1989) and Riquarts (1981), as shown

in Table 6.1, where the maximum liquid velocity at the column axis is expressed as a function of superficial gas velocity, column diameter and so on.

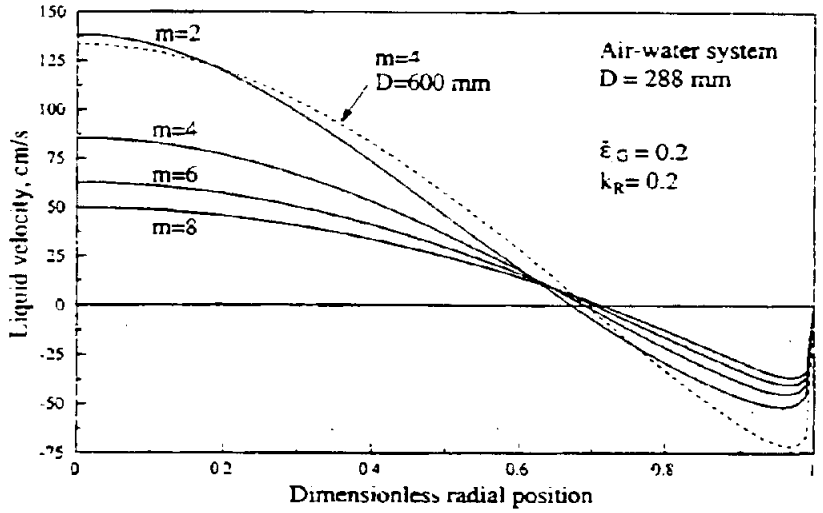


**Figure 6.13** Effect of $m$ on $u_l$.

**Table 6.1** Correlations of the maximum liquid velocity.

| Correlation | Reference |
|---|---|
| $u_{l0} = 0.21(gD)^{0.5}(u_G^3/g\mu_L)^{1/8}$ | Riquarts (1981) |
| $u_{l0} = 0.737(\Delta\rho g D u_G/\rho_L)^{1/3}$ | Kraume and Zehner (1989) |
| $u_{l0} = 6.8u_G^{0.5}D^{0.28}$ | Koide *et al.* (1979) |

*6.4.2.3 Effect of liquid viscosity*

In the literature, very little work has been found regarding the effect of liquid viscosity on the liquid circulation in bubble columns. However, Riquarts (1981) has obtained $u_{l0} \sim \mu_L^{-0.125}$, as shown in Table 6.1. In the present work, the effect of liquid viscosity on the liquid circulation has been calculated, as shown in Figure 6.14. A lower liquid viscosity causes a stronger liquid circulation when all other conditions are identical. Comparing the predicted results in Figure 6.14 with the correlation of Riquarts (1981) in Table 6.1, it can be found they have similar trend of change and are roughly in agreement. For example, the predicted $u_{l0}$ decreases from 85.5 cm/s to about 69 cm/s as $\mu_L$ increases from 0.001 Pa·s to 0.01 Pa·s. This indicates $u_{l0} \sim \mu_L^{-0.093}$. When $\mu_L$ increases from 0.01 to 0.1 Pa·s, $u_{l0}$ decreases to about 50 cm/s, and this gives $u_{l0} \sim \mu_L^{-0.14}$.

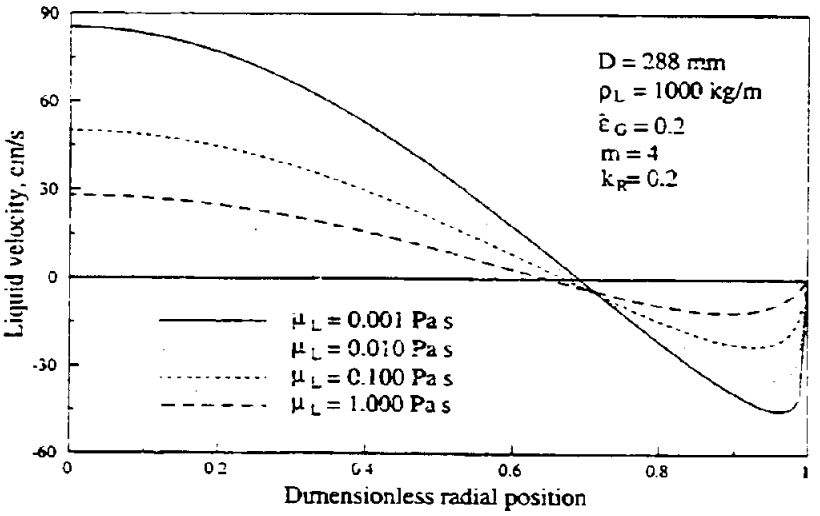


**Figure 6.14** Effect of $\mu_L$ on $u_l$.

The position of the velocity inversion point changes with liquid viscosity. The higher the liquid viscosity, the closer to the center axis the inversion point. This is also found from experimental results (Rietema and Ottengraf, 1970; Walter and Blanch, 1983).

*6.4.2.4 Effect of overall gas holdup*

Figure 6.15 shows the effect of the overall gas holdup, $\bar{\varepsilon}_G$, on the liquid velocity profiles in the air-water system. It can be seen that the liquid circulation increases with the overall gas holdup when all other conditions are kept constant. This implies that the liquid circulation in a non-coalescing system will be stronger than that in a coalescing system, since the overall gas holdup of a non-coalescing system is usually larger than that of a coalescing system (under the same conditions, more large bubbles exist in a coalescing system. The larger the bubbles. usually the less the residence time in liquid). This phenomenon is supported by the experimental results of Menzel *et al.* (1990), as shown in Figure 6.9 and Figure 6.10. The physical properties were nearly equal in both the non-coalescing system (0.22 *wt.%* propanol-water) and the coalescing system (water), but the former had higher gas holdup.

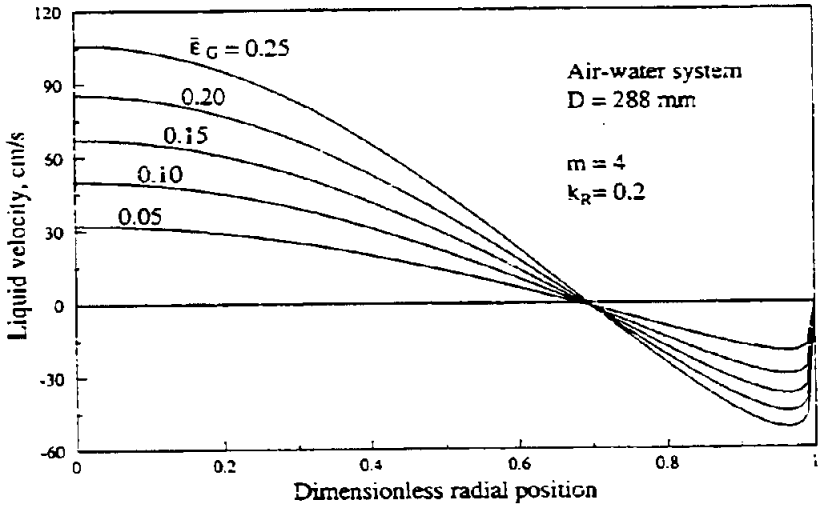


**Figure 6.15** Effect of $\bar{\varepsilon}_G$ on $u_l$.

It can also be concluded that a higher superficial gas velocity normally causes a stronger liquid circulation, since the overall gas holdup usually increases with the superficial gas velocity. Table 6.1 lists three empirical or semi-theoretical correlations for the maximum liquid velocity dependent on the superficial gas velocity. The table shows that the maximum liquid velocity changes with different powers of the superficial gas velocity. The difference may be the result of uncertainties in the relationship between the superficial gas velocity and the overall gas holdup. For instance, for a coalescing system, there may exist a transition flow regime. Passing this regime, when increasing superficial gas velocity, may lead to a decrease in overall gas holdup or may make it remain constant.

#### 6.4.2.5 *Comparison with reported experimental results*

Data generated by the two-fluid liquid circulation model has been compared to the reported experimental results also used in the comparisons for the pseudo-homogeneous model. The two-fluid model is also in good agreement with the experimental data. However, for this model, the tuning of $m$ is usually avoided and the $m$ taken directly from the experimental data can be used. Only an example is given in Figure 6.16 for the data of Menzel *et al.* (1990). This because other authors (*e.g.* Franz *et al.*, 1984) did not give the data of $\bar{\varepsilon}_G$ and $m$. (In the comparisons with their data, $u_{l0}$ was used and $m$ was tuned to the velocity profile data, but $m < 8$ was usually obtained)

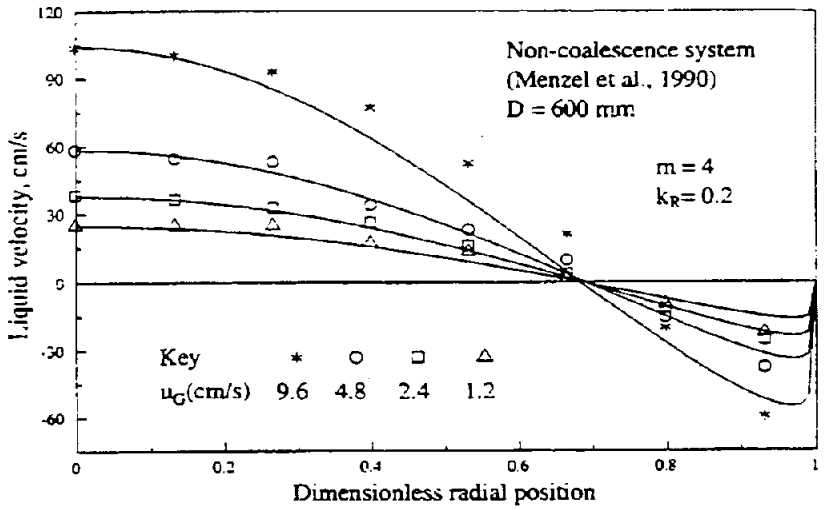


**Figure 6.16** Comparison with the data of Menzel *et al.* (1990) in a non-coalescing system, for the two-fluid model.

## 6.5 Conclusion

The pseudo-homogeneous fluid concept and the two-fluid concept have been clarified for modeling the liquid circulation in bubble columns. Two models have been developed using the two different concepts. Both are based on a turbulent viscosity distribution in single-phase pipe flows and an empirical correlation for describing the radial gas holdup distribution in bubble columns. Analytical expressions are obtained that are easy and effective to use for the prediction of liquid velocity profiles for low viscosity fluids, which avoids solving boundary value differential equation systems. The pseudo-homogeneous model is the simpler, but the gas holdup distribution parameter, $m$, needs to be optimized. The two-fluid model can use the value of $m$ determined from experimental data. Both models can give good predictions for liquid velocity profiles, compared to the experimental data available in the literature.

Since the two models both include the relative influence of the eddy and the molecular viscosities over the whole cross-section of a column, they are expected to be useful also for high viscosity fluids. This has experimentally been confirmed. It has been shown that the effect of the molecular viscosity on the flow in bubble columns is not negligible even for low viscosity fluids. The successful use of the turbulent viscosity distribution for single-phase flows to bubble columns also implies that there exists a strong analogy between the transport properties in multi-phase systems and single-phase systems.

However, like for all other liquid circulation models, an empirical gas holdup distribution, $\varepsilon_{G0}(1-c\phi^m)$, is still needed and the gas holdup distribution parameter, $m$ (the other parameter, $c$, can be set to unity), has to be determined or tuned. In fact, this distribution function may show deviations from the real gas holdup profiles. In addition, the values of the parameter, $m$, are known to depend on both the flow regime and the system. Hence, this function should preferably be avoided or the parameter, $m$, determined by modeling.

This may be realized according to the principle of energy minimization in a system. That is, it can be done by minimizing the rate of energy dissipation per unit reactor volume, as expressed by Geary and Rice (1992):

$$\varepsilon_v = \frac{2\rho_L \nu_L u_{l0}^2}{R^2} \int_0^1 (1-\varepsilon_G)\left(\frac{\nu_t}{\nu_L}+1\right)\left(\frac{d\bar{u}_l}{d\phi}\right)^2 \phi\, d\phi \qquad (6.31)$$

On the other hand, this may also be done using the analogy between the turbulent properties of single- and multi-phase flows. For example, it can be suggested that the dimensionless maximum liquid velocity in bubble columns, $u_{l0}/\hat{u}$, is related to the wall shear stress in the same way as in single-phase pipe flows. This would give

$$\frac{u_{l0}}{\hat{u}} = 2.505\ln(R^+)+5.06 \qquad (6.32)$$

This work may be done in the future.